This article has been accepted for publication in a future issue of this journal, but has not been fully edited. Content may change prior to final publication. Citation information: DOI 10.1109/TII.2017.2778346, IEEE Transactions on Industrial Informatics

Control of Solar Photovoltaic Integrated Universal Active Filter Based on Discrete Adaptive Filter

Sachin Devassy, *Member, IEEE* and Bhim Singh, *Fellow, IEEE*

***Abstract*—In this work, a novel technique based on adaptive filtering is proposed for the control of three phase universal active power filter with a solar photovoltaic array integrated at its DC-bus. Two adaptive filters along with a zero crossing detection technique, are used to extract the magnitude of fundamental active component of distorted load currents, which is then used in estimation of reference signal for the shunt active filter. This technique enables extraction of active component of all three phases with reduced mathematical computation. The series active filter control is based on synchronous reference frame theory and it regulates load voltage and maintains it in-phase with voltage at point of common coupling under conditions of voltage sag and swell. The performance of the system is evaluated on an experimental prototype in the laboratory under various dynamic conditions such as sag and swell in voltage at point of common coupling, load unbalancing and change in solar irradiation intensity.**

***Index Terms*—power quality, universal active power filter, adaptive filtering, photovoltaic system, maximum power point tracking, quadrature signal generation.**

NOMENCLATURE

v_{Ma}, v_{Mb}, v_{Mc}	Grid voltages
Z_a,Z_b,Z_c	Grid impedances
v_{sa}, v_{sb}, v_{sc}	PCC phase voltages
V_s	PCC voltage magnitude
$v_{sab}, v_{sbc}, v_{sca}$	PCC line voltages
u_{sa}, u_{sb}, u_{sc}	PCC voltage templates
v_{la}, v_{lb}, v_{lc}	Load phase voltages
$v_{lab}, v_{lbc}, v_{lca}$	Load line voltages
$v_{sea}, v_{seb}, v_{sec}$	series active filter phase voltages
V^*_{Ld}, V^*_{Lq}	Reference load voltages in d-q domain
V_{Ld}, V_{Lq}	Load voltages in d-q domain
V_{sd}, V_{sq}	PCC voltages in d-q domain
V^*_{sed}, V^*_{seq}	Series active filter reference voltages in d-q domain
V_{sed}, V_{seq}	Series active filter voltages in d-q domain
$v_{sea}*, v^*_{seb}, v^*_{sec}$	Control signals for series active filter
i_{sa}, i_{sb}, i_{sc}	Grid line currents
I^*_s	Reference grid current magnitude
$i^*_{sa}, i^*_{sb}, i^*_{sc}$	Reference grid currents
$i_{SHa}, i_{SHb}, i_{SHc}$	Shunt active filter line currents
i_{La}, i_{Lb}, i_{Lc}	Load line currents
ϕ	Load angle
I_{pv}	Solar PV array current
V_{pv}	Solar PV array voltage
V_{dc}	DC-link voltage
ω_s	resonant frequency of filter
T_s	Controller sampling time
n	sampling instant
q	Quadrature shift operator
I_{pvg}	grid current equivalent to PV power
T_m	MPPT sampling time
δV_{pv}	MPPT perturbation step size

ABBREVIATION

PV	Solar Photovoltaic
PCC	Point of Common Coupling
VSC	Voltage source converter
$PV-UAPF$	Solar photovoltaic integrated universal active power filter
$SOGI$	Second order generalized integrator
$FACTS$	Flexible AC transmission system
FPS	Fundamental positive sequence
DSC	Delayed signals cancellation
DFT	Discrete Fourier transform
$ADALINE$	Adaptive linear element
LMS	Least mean square
LMF	Least mean fourth
$UAPF$	Universal active power filter
$UPFC$	Unified power flow controller
$MPPT$	Maximum power point tracking
DSP	Digital signal processor
LPF	Low-pass filter
ZCD	Zero crossing detection
S/H	Sample and Hold
PI	Proportional-Integral
PLL	Phase locked loop
THD	Total harmonic distortion

I. INTRODUCTION

THERE has been an increased proliferation of clean energy systems based on solar and wind energy in mordern distribution system. However, due to their intermittent nature, voltage fluctuations have become a major issue in low voltage distribution system [1]. Along with this, the advancement in semi-conductor technology has led to the widespread use of sophisticated power electronic systems like computer power supplies, switched mode power supplies, variable frequency drives, servers, etc. These systems are energy efficient but draw highly nonlinear current from the supply system. Moreover, this increasing sophistication has led to an increased sensitivity to voltage disturbances. The nonlinear currents drawn by power electronic loads, lead to increased losses in distribution transformers, distortion of voltage at the point of common

This article has been accepted for publication in a future issue of this journal, but has not been fully edited. Content may change prior to final publication. Citation information: DOI 10.1109/TII.2017.2778346, IEEE Transactions on Industrial Informatics

coupling (PCC), etc. [2], [3]. Thus the future systems demand clean energy along with improved power quality.

The integration of clean energy generation along with active filtering, mitigates power quality problems in distribution system while also reducing dependance on fossil fuels thus leading to improved quality of environment [4]. Renewable energy integration with flexible AC transmission systems (FACTS) devices such as unified power flow controller (UPFC) has been discussed in [5], [6]. These devices are mainly used for improving stability of the power system while integrating large PV farms. Primarily, FACTS devices such as UPFC is used in transmission systems. The shunt compensator is connected at the primary feeder and series compensator is connected at the secondary feeder. Moreover, only simulation results have been provided in the literature regarding operating of FACTS devices with renewable energy systems. However, renewable energy integration with active power filter is used in distribution systems wherein in load current compensation is a major requirement. The proposed system compensates for load current harmonics, protects sensitive loads from voltage sags/swells and also injects active power from PV array. While the structure of a active power filter is similar to FACTS devices, the shunt compensator of active filter is at load side to mitigate load current quality issues while a series active filter is at supply side. This structure has the benefit of lower rating of series active filter as current flowing to the series active filter is balanced and sinusoidal. A comparison between FACTS devices and proposed system is presented in Table I.

TABLE I
COMPARISON BETWEEN FACTS DEVICES WITH RENEWABLE ENERGY INTEGRATION AND PV-UAPF

SL. No	FACTS with Renewable Energy System	PV-UAPF System
1	Employed in Transmission system	Employed in Distribution Systems
2	For Integration of PV and wind farms	Integration of distributed generation sources
3	Main function is power system stability	Main function is power quality improvement
4	No harmonic current compensation	Load harmonic current compensation present

Primarily, research has been done in the integration of power quality along with shunt connected renewable energy systems [7]. However, the shunt connected topologies cannot regulate voltage at the load side and maintain grid current at unity power simulataneously, as voltage regulation by shunt compensator requires reactive power [8].Moreover, the voltage compensation capability of the shunt compensator, depends upon the impedance of the supply system which directly affects the rating of the shunt compensator. Universal active power filter has both shunt and series filters and protects sensitive nonlinear loads against voltage sags/swells at PCC side along with improving the grid current quality. Due to the increased sags/swells in PCC voltages owing to large scale integration of renewable energy sources, which are intermittent, there has been increased research on renewable energy systems integrated with universal active power filters [9]. Solar PV integrated universal active power filter (PV-UAPF) provides a complete solution for integrating clean energy sources along with improving power quality of distribution systems [10], [11]. Though there is extra cost incurred due to the extra series converter required in case of PV-UAPF, this cost is justified in case of systems which have highly sensitive loads such as semiconductor industries, PLCs, adjustable speed drives etc. where any loss of production due to power quality issues can lead to huge economic losses.

Reference signal generation is one of the most important factors affecting the performance of active filters. Two main reference signals for PV-UAPF system are the load voltages and grid currents. In distribution systems, the load currents are highly distorted and also subjected to unbalancing conditions, while voltage disturbances are mainly sag/swell in PCC voltages. Fast and accurate estimation of fundamental frequency load current active component particularly under unbalancing conditions is of prime importance in control of PV-UAPF system. Conventional algorithms for reference signal estimation include methods based on p-q theory [12] and d-q theory [13]. However, the performance of these methods deteriorate under unbalanced load conditions. This is because the cut-off frequency of low pass filters used in these techniques would have to be kept very low to filter out double harmonic components present during load unbalanced conditions. This affects the dynamic performance of the system.

Some advanced control techniques based on adaptive notch filters have been proposed in [14], [15]. In these techniques, an adaptive notch filter is used in each phase of a system to extract fundamental load active current component. Though they have good dynamic response, the computational burden is higher. Another technique for extracting the fundamental component of distorted signals, is by the use of second order generalized integrator (SOGI) band pass filters. In [16], a fundamental positive sequence (FPS) extractor based on SOGI has been used to detect FPS components of PCC voltage. Recently use of delayed signal cancellation (DSC) based method for extraction of fundamental components have been proposed in [17]. In this technique, multiple delayed signal cancellation blocks are cascaded together for perfect cancellation of harmonics and extraction of fundamental component of distorted signal. This method is insensitive to minor variations in frequencies and presence of DC-offset in sensed signals, which comes at cost of increased computational burden.

Other techniques for extraction of fundamental component include frequency domain techniques such as those based on discrete Fourier transforms (DFT) such as sliding DFT, wavelet transforms etc. [18], [19]. However, their computational burden is very high and are more suitable for power quality monitoring operation rather than for real-time applications. Another approach in extraction of fundamental active component of load, is by the use of ADALINE structure. In ADALINE based methods, the output is adapted based on adaptive filter theory such as least mean square (LMS), least mean fourth (LMF), recursive least squares, affine-projection etc. [20], [21].

In this work, an adaptive filer based technique is proposed for control of three phase-three wire PV integrated UAPF sys-

This article has been accepted for publication in a future issue of this journal, but has not been fully edited. Content may change prior to final publication. Citation information: DOI 10.1109/TII.2017.2778346, IEEE Transactions on Industrial Informatics

tem. The adaptive filter considered is a fourth order quadrature signal generator [22]. Two adaptive filters are used to estimate the fundamental positive sequence components of distorted load currents. These positive sequence components are then used to estimate reference signal for the shunt active filter of PV-UAPF system. The proposed method has reduced computational burdern and has good dynamic response. The series active filter of the PV-UAPF is controlled using synchronous reference frame theory based technique to compensate for voltage sags/swells at the PCC. A maximum power point tracking (MPPT) algorithm is used to operate PV array at its peak power point [23]. Since this is a single stage system, the MPPT algorithm generates the reference DC-link voltage. The main advantages of the system are as follows,

- Multi-functional system providing pollution free clean energy based on solar PV power along with clean power quality.
- The power generated from PV array, supplies load power thus reducing active power demand from supply system.
- The sampling of positive sequence currents obtained by adaptive filter based on zero crossing of load voltage, enables estimation of magnitude of active component of all phases with one sampling.
- The proposed system protects sensitive loads from PCC voltage sags/swell while maintaining grid current within IEEE 519 standard.
- The system performance is robust under various disturbances in the load, voltage sags/swells at the PCC and solar irradiation.

The performance of PV-UAPF system is evaluated under both steady state and dynamic conditions using an experimental prototype. The steady state performance of the system is verified to check its compliance with IEEE-519 standard. The dynamic performance of the PV-UAPF is evaluated under conditions such as voltage sag/swell at PCC, load disturbances and change in solar irradiation.

II. System Configuration

Fig. 1 shows the configuration of a PV-UAPF system. This a three phase system consisting of a shunt active filter and series active filter with a common DC-bus. The shunt active filter is interfaced near the nonlinear load whereas the series active is interfaced in series with the PCC. Other major components of the system include interfacing inductors, ripple filters and injection transformers. The PV array is coupled directly to the DC-bus of PV-UAPF system. A diode is used while integrating the PV array with PV-UAPF to prevent reverse power flow into PV array. The detailed design methodology of PV-UAPF is given in [2].

The phasor representation of operation of PV-UAPF is given in Fig.2. The signals under nominal condition have subscript '1' while signals under PCC voltage sag condition are represented with subscript '2' . The load voltage (V_{L1}) and PCC voltage (V_{s1}) are equal under nominal conditions. The load current (I_{L1}) lags behind V_{L1} with a phase angle ϕ. During sag condition, the series active filter injects a voltage (V_{SE}) in phase with the PCC voltage (V_{s2}) to maintain load voltage

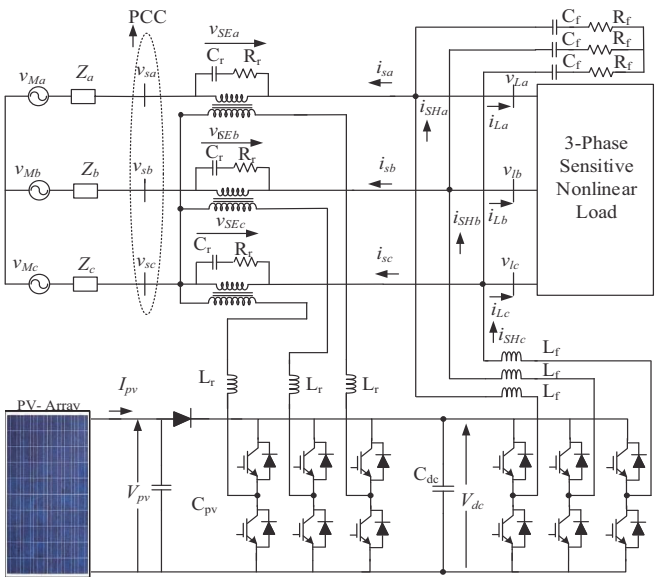

Fig. 1. System Configuration of Solar Photovoltaic Integrated Unified Active Power Filter

(V_{L2}) in same magnitude and phase as that of nominal PCC voltage (V_{s1}). The shunt active filter current (I_{SH1}, I_{SH2}) is a combination of load reactive power and current corresponding to PV array power injection (I_{pvg1}, I_{pvg1}). The PV power generation is more than the load active power demand, and consequently the excess power is fed into the grid.

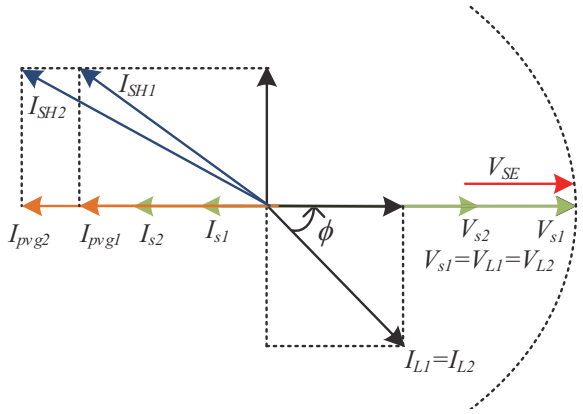

Fig. 2. Phasor Representation of PV-UAPF system operating with a linear load

III. System Control

The major function in control of PV-UAPF system is estimation of reference signals for the shunt and series active filters. Apart from this, the system also has to extract maximum power available from the PV array. The detailed description of the PV-UAPF control structure is explained as follows.

A. Control of Shunt Active Filter

The shunt active filter control is presented in Fig. 3(b). The primary task in the control of a shunt active filter is generation of reference currents. In this work, the shunt active filter is

This article has been accepted for publication in a future issue of this journal, but has not been fully edited. Content may change prior to final publication. Citation information: DOI 10.1109/TII.2017.2778346, IEEE Transactions on Industrial Informatics

controlled using indirect current control wherein the reference for the shunt active filter is the grid current, which should only contain fundamental and active power component. The shunt active filter control blocks involve three sub-blocks i.e. DC-nus control block, load active current evaluation block and PV feed forward block. Two adaptive filters are used to extract the fundamental positive sequence components of the load current.

The basic structure of adaptive filter is shown in Fig. 3(a).

This basic structure is a fourth order system consisting of a quadrature signal generator with a gain K and resonant frequency ω_s. The input to the filter is a sinusoidal input given as,

$$x(nT_s) = X_m sin(\omega_c kTs + \phi_c) \tag{1}$$

where T_s is sampling time of the system, X_m is magnitude of sinusoidal wave

For the input $x(nT_s)$, the adaptive filter provides two signals which are in quadrature with each other,

$$x_1(n+1) = -x_1(n) + \mu(n) \tag{2}$$

$$qx_1(n+1) = qx_1(n) + tan(\frac{\omega_s T_s}{2})\mu(n) \tag{3}$$

where

$$\mu(n) = \frac{tan(\frac{\omega_s T_s}{2})(K_s(x(n) + x(n+1) - 2qx_1(n)) + 2x_1(n)}{1 + tan(\frac{\omega_s T_s}{2})(K_s + tan(\frac{\omega_s T_s}{2}))} \tag{4}$$

where q is a quadrature shift operator.

The frequency adaptive law of the system is given as,

$$\omega_s(n+1) = \omega_s(n) - \gamma(tan(\frac{\omega_s(n) T_s}{2})(x(n) - x_1(n))qx_1(n) \tag{5}$$

Since $\omega_s(n)$ is time adaptive, the adaptive filter is a non-linear filter. The factor K_s is chosen based on compromise between steady state accuracy and dynamic performance. In this work,K_s is chosen as 0.5. The value of γ used in the system is 0.0002. The detailed description regarding the stability analysis and parameter selection of filter are presented in [22].

The frequency tracking capability of the adaptive filter is shown in Fig.4. The signal frequency changes from 50Hz to 48Hz and back to 50Hz. The adaptive filter is able to track the step change in frequency within 0.1s.

The three phase grid currents are converted to $\alpha - \beta$ domain using magnitude invariant Clarke's transform. The α component is given to adaptive filter block 1 and β component is given to adaptive filter block 2. Each adaptive filter gives fundamental component $(i_{L\alpha 1}, i_{L\beta 1})$ and its quadrature shifted versions $(qi_{L\alpha 1}, q_{L\beta 1})$. The fundamental positive sequence component in α axis is obtained as,

$$i_{L\alpha 1^+} = i_{L\alpha 1} - qi_{L\beta 1} \tag{6}$$

Once the fundamental component of load current is obtained, the magnitude of active component (I_{La}) is obtained by sampling the $i^+_{L\alpha 1}$ at the zero crossing of the β component

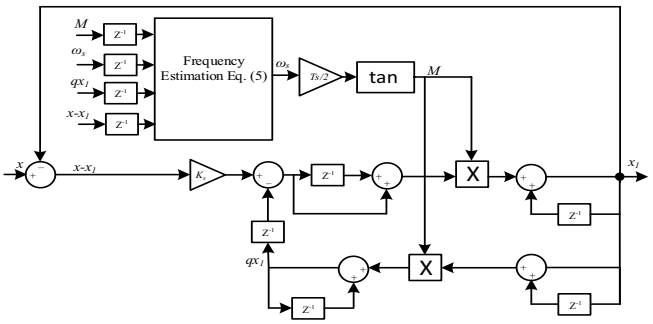

(a) Configuration of Frequency Adaptive Filter

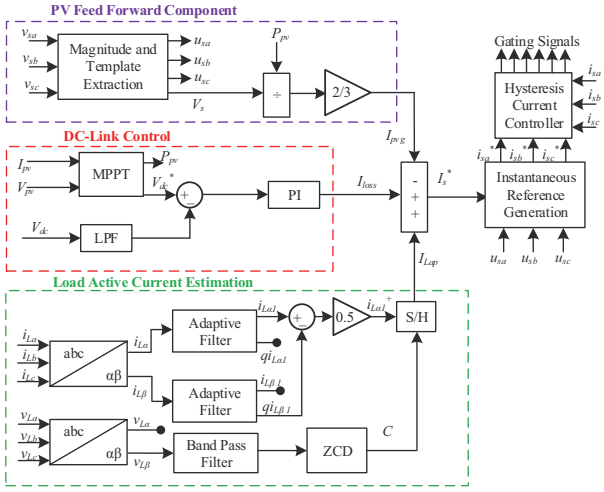

(b) Control Configuration of Shunt Active Filter

Fig. 3. Adaptive Filter Based Control of Shunt Active filter

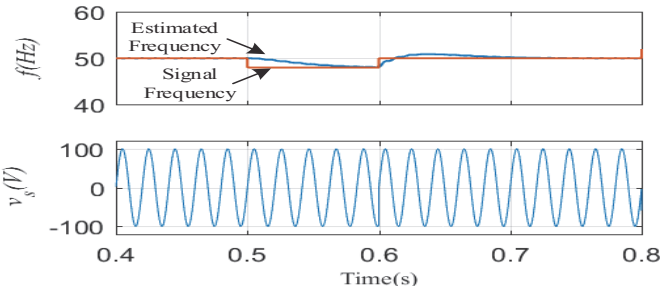

Fig. 4. Frequency Tracking Response of the Adaptive Filter

of the load voltage component. Since the magnitude invariant transformation is used, the sampled α component of the positive sequence currents, is the average active component component of load current in each phase.

The DC-bus control block maintains the DC-link voltage of the PV-UAPF. It consists of a proportional-integral (PI) controller. The input to PI controller is error between reference voltage and sensed DC-bus voltage. The DC-bus voltage is filtered using a low pass filter to eliminate noise present in DC-bus voltage.

The reference for the PI controller is obtained using a MPPT controller. The task of MPPT controller is to operate the PV

This article has been accepted for publication in a future issue of this journal, but has not been fully edited. Content may change prior to final publication. Citation information: DOI 10.1109/TII.2017.2778346, IEEE Transactions on Industrial Informatics

array at its maximum power point. The PV array is designed such that the maximum power point of PV array is also the operating DC-link voltage of PV-UAPF system. In this work, a perturb and observe (P&O) based MPPT controller is used due to its simplicity and ease of implementation. The perturb and observe algorithm is a hill climb search technique where, the reference voltage is updated based on difference in power between present and past sampling instants. The P&O algorithm searches for the peak of P-V curve by checking the slope on P-V curve dP_{pv}/dV_{pv}. The operating voltage of PV array, V_{pv} is perturbed with a small step change depending upon the sign of slope.

Two important parameters in MPPT operation, are the MPPT sampling time (T_m) and perturbation step size ($\delta V_p v$). A smaller step size results in smaller oscillation around MPP point, however, it results in poor dynamic response. Similarly, a large sampling time enables the algorithm to track MPP without getting disturbed by noise. However, larger sampling time consequently results in poor dynamic response. A detailed discussion of selection of T_m and δV_{pv} is given in [23] and values used in this work are given in Table. II.

The reference voltage generated through MPPT algorithm is compared sensed DC-bus voltage in a PI controller. The control law for the DC-bus controller is given as,

$$I_{loss}(n) = I_{loss}(n-1) + K_p \Delta e_{vdc} + K_i e_{vdc}(n) \quad (7)$$

where I_{loss} is the output of PI controller, which is also the loss component of PV-UAPF, K_p and K_i are the gains of PI controller and Δe_{vdc} is the difference in DC-bus voltage error between the present and past sampling time. e_{vdc} is the DC-bus voltage error.

The PV feed forward component block estimates the equivalent grid current magnitude generated due to PV array active power and is obtained as follows,

$$I_{pvg} = \frac{2}{3}\frac{P_{pv}}{V_s} \quad (8)$$

where P_{pv} is power obtained from PV array, V_s is magnitude of PCC voltage.

The magnitude of PCC voltage V_s and the PCC voltage in-phase templates are extracted using the following equations:

$$V_s = \sqrt{\frac{2}{3}(v_{sa}^2 + v_{sb}^2 + v_{sc}^2)} \quad (9)$$

$$u_{sa} = \frac{v_{sa}}{V_s}, u_{sb} = \frac{v_{sb}}{V_s}, u_{sc} = \frac{v_{sc}}{V_s}, \quad (10)$$

The magnitude of reference current for the shunt active filter, is obtained as follows,

$$I_s^* = I_{Lap} + I_{loss} - I_{pvg} \quad (11)$$

The reference magnitude is multiplied with templates of PCC voltages to generate instantaneous reference grid currents $(i_{sa}^*, i_{sb}^*, i_{sc}^*)$ as,

$$i_{sa}^* = I_s^* \times u_{sa}, i_{sb}^* = I_s^* \times u_{sb}, i_{sc}^* = I_s^* \times u_{sc}, \quad (12)$$

A hysteresis current controller, after comparing reference signals with the sensed signals, generates appropriate pulses for the gating circuitry of shunt active filter.

B. Control Configuration of Series Active Filter

Fig. 5 gives the series active filter control block diagram. The PCC voltages (v_{sa}, v_{sb}, v_{sc}) and load voltages (v_{La}, v_{Lb}, v_{Lc}) are converted to d-q domain using phase information of PCC voltages for d-q transformation. The load voltages are in-phase with PCC voltages as the series active filter injects voltages in-phase with PCC voltages. Hence the direct component of reference load voltage, is the magnitude of reference load voltage (V_{Ld}^*) and quadrature component of reference load voltage (V_{Lq}^*) is zero.

The direct component of reference series active filter voltage, is obtained as the difference between V_{Ld}^* and V_{sd}^*. The difference between V_{Ld} and V_{sd} gives direct component of series active filter voltage. Similar operation is done for the quadrature components.

$$V_{sed}^* = V_{Ld}^* - V_{sd}, V_{sed} = V_{Ld} - V_{sd} \quad (13)$$

$$V_{seq}^* = V_{Lq}^* - V_{sd}, V_{seq}^* = V_{Lq} - V_{dq} \quad (14)$$

The error between (V_{sed}^*, V_{seq}^*) and $((V_{se}, V_{seq})$ are passed through PI controller to generate control signals for the series active filter. The control signals are then converted to stationary frame and then passed through PWM modulator to generate switching signals for controlling the series active filter.

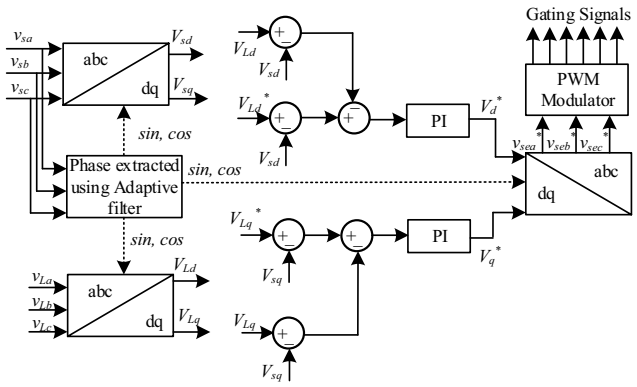

Fig. 5. Control Configuration of Series Active Filter

IV. Results

The performance of adaptive filter based PV-UAPF system is evaluated on an experimental prototype developed in the laboratory. The solar array power is obtained using a solar array simulator and the active filters have been realized by using two set of three-leg IGBT stacks having common DC-bus. The load consists of a three phase bridge rectifier with an highly inductive load. A DSP-dSPACE MicrolabBox rapid prototyping controller is used for controlling the prototype. A four-channel digital storage oscilloscope (Agilent DSO7014A with a bandwidth of 100 MHz) is used to capture the waveforms during dynamic conditions. Table II gives the detailed experimental system parameters and ratings. A photograph of the prototype is presented in Fig.6

This article has been accepted for publication in a future issue of this journal, but has not been fully edited. Content may change prior to final publication. Citation information: DOI 10.1109/TII.2017.2778346, IEEE Transactions on Industrial Informatics

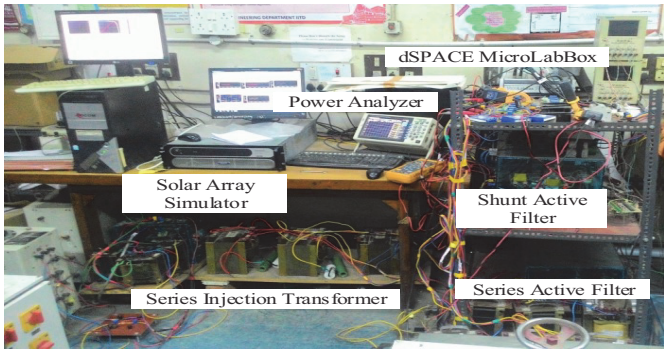

Fig. 6. Laboratory Prototype of PV-UAPF System

TABLE II
EXPERIMENTAL PARAMETERS

Parameter	Values
PCC voltage	v_s = 220 V, f = 50 Hz
Grid Impedance	Z_a, Z_b, Z_c=0.7 Ω,477μH
Nonlinear Load	Rectifier with R-L: 1.12 kW
DC-bus Voltage	V_{dc} = 360 V
DC-bus Capacitor	C_{dc} = 3.3 mF
Shunt Active Filter Inductor	L_s = 4 mH
Series Active Filter Inductor	L_{se} = 0.5 mH
MicrolabBox Sampling Time	T_s = 33.33 μs
DC-bus PI contoller	K_p = 0.8, K_i = 0.2
Series Compensator PI controller	K_{pD} = 2; K_{ID} = 400
	K_{pQ} = 2; K_{IQ} =400
LPF cut off frequency	f_{LPF} = 10 Hz;
PV Array	P = 4.8 kW,
	V_{oc} = 415 V, I_{sc} = 14 A
	V_{mpp} = 360.23 V, I_{mpp} = 13.329 A
MPPT Parameters	T_m= 0.04s ,δV_{pv}= 0.5 V

A. Internal Signals for PV-UAPF System Control

Fig. 7 presents the performance of the adaptive filters in extraction of fundamental positive sequence component of load currents. The main waveforms recorded are phase 'b'

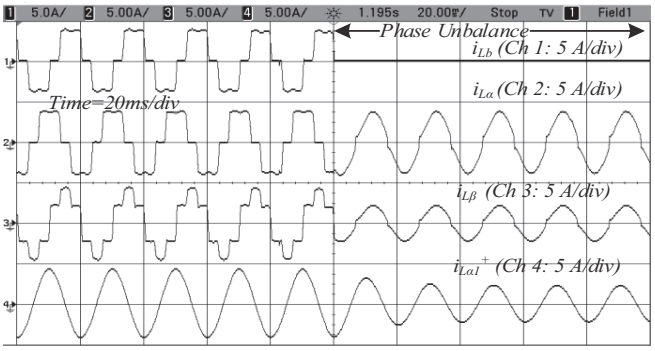

Fig. 7. Salient Signals in Extraction of Fundamental Positive Sequence Load Current using Adaptive Filter

load current (i_{Lb}), load current in $\alpha - \beta$ domain ($i_{L\alpha}$, $i_{L\beta}$) and α component of fundamental positive sequence load current $i^{+}_{L\alpha 1}$. The load current is nonlinear and load of phase 'b' is removed, creating an unbalanced load condition. The adaptive filter technique is able to extract fundamental positive sequence component of load current within a one-cycle. Fig.

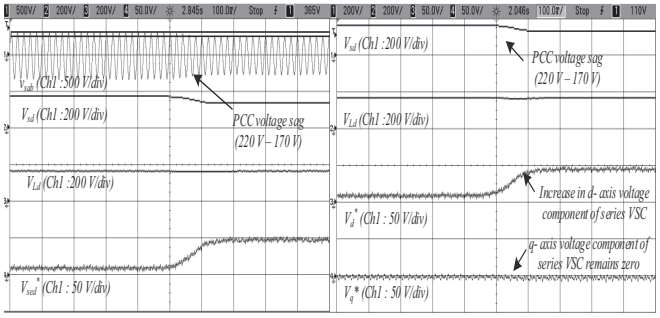

(a) Reference Generation of Series Active Filter in d-q Domain (b) Control Signal Generation of Series Active Filter in d-q Domain

Fig. 8. Salient Signals in Series Active Filter Control

8 presents the series active filter control signals. The signals captured are v_{sab}, V_{sd}, V_{Ld} and V_{sed}. The internal signals are recorded during dynamic condition when there is a sag in PCC voltage. It can be observed that during sag, the d-axis component of PCC voltage reduces, however, the load voltage component remains at same level. An appropriate voltage is injected by the series active filter to maintain the load voltage at its desired regulation level.

From Fig. 8(b), it can be noted that the series active filter injects only d-axis component voltage while the q-axis component remains zero. This means that the PCC voltage and series compensator voltage are in-phase, which results in load voltage also being in-phase.

B. Performance of PV-UAPF during Steady State Condition

The steady state PV-UAPF system capability in load compensation and voltage regulation, is evaluated under conditions of nominal conditions, PCC voltage sags/swells.

The steady state waveforms of a phase of PV-UAPF are given in Fig. 9. The recorded signals are v_{sa}, i_{sa}, v_{La} and i_{La}. In order to present both load side and PCC side information, only phase 'a' signals are recorded. The PCC current contains only fundamental active component while the load current is of a nonlinear quasi square wave shape. The voltage at load side is regulated and maintained in-phase with voltage of PCC during all conditions.

Figs. 10,11,12 show the behavior of PV-UAPF system under nominal, sag and swell conditions. These results and harmonic spectra are recorded using power analyzer (HIOKI3390). The relation between the power analyzer signals with system signals are given in TableIII.

It can be observed that though the THD of the load current is approximately 28%, the grid current THDs are maintained below 5%. The grid current meets specifications of IEEE-519 standard. Moreover, the power factor at PCC is approximately unity. The voltage at the load side is maintained at the desired RMS value of 220 V even though the voltage at PCC undergoes variation from 170 V during sag condition to 270 V during swell condition. The total power ($P12$) at the PCC side is negative due to the fact that the surplus PV array power is being fed into the PCC.

This article has been accepted for publication in a future issue of this journal, but has not been fully edited. Content may change prior to final publication. Citation information: DOI 10.1109/TII.2017.2778346, IEEE Transactions on Industrial Informatics

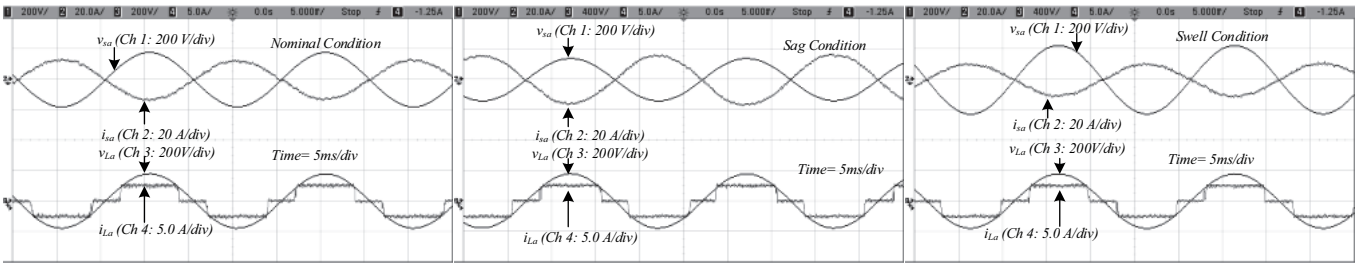

(a) Steady State Per Phase Voltage and Current Signals During Nominal Condition

(b) Steady State Per Phase Voltage and Current Signals During Sag Condition

(c) Steady State Per Phase Voltage and Current Signals During Swell condition

Fig. 9. Steady State Per Phase Signals of PCC and Load Side in a PV-UAPF Compensated System

TABLE III
RELATION BETWEEN POWER ANALYZER CHANNELS AND CORRESPONDING SYSTEM SIGNALS

Displayed Signals	Load side/PCC side signals
Ch 1, Ch 2	PCC side signals ($V_{sab}, V_{scb}, I_{sa}, I_{sc}$)
Ch 3, Ch 4	Load side signals ($V_{Lab}, V_{Lcb}, I_{La}, I_{Lc}$)
P12, Q12, S12	Power Components in PCC side
P34, Q34, S34	Power Components in Load side
$\lambda 12$	Power Factor at PCC side
$\lambda 34$	Power Factor at load side
f	Frequency of the supply system

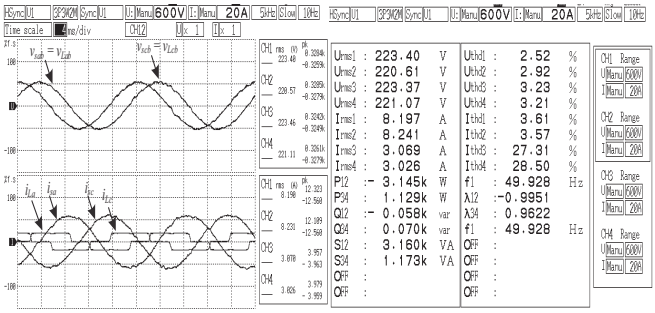

(a) PCC and Load Signals during Nominal Condition

(b) Performance Parameters of Compensated System during Nominal Condition

Fig. 10. PV-UAPF Response under Nominal Condition

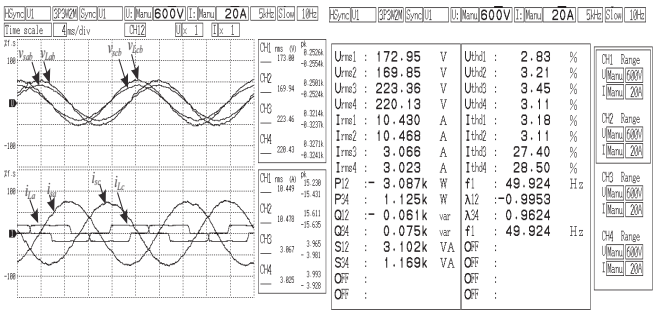

(a) PCC and Load Signals during PCC Voltage Sag

(b) Performance Parameters of Compensated System during PCC Voltage Sag

Fig. 11. PV-UAPF Response under Sag Condition

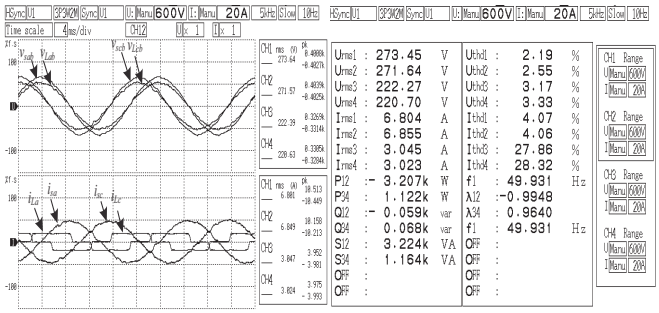

(a) PCC and Load Signals during PCC Voltage Swell

(b) Performance Parameters of Compensated System during PCC Voltage Swell

Fig. 12. PV-UAPF Response under Swell Condition

C. Dynamic Performance of PV-UAPF System

The dynamic performance of the adaptive filter based PV integrated universal active filter is evaluated by subjecting the system to various disturbances such as sag and swell in the voltage at PCC, load unbalancing and variation of solar irradiation intensity. The performance of the PV-UAPF system under PCC voltage disturbances are given in Fig. 13. The signals captured are PCC voltage (v_{sab}), load voltage (v_{Lab}), series active filter voltage (v_{seab}) and line current (i_{sa}). Fig. 13(a) shows the performance of the system under sag condition when v_{sab} dips from its nominal voltage to 170 V, while Fig. 13(b) shows the performance of the system under PCC voltage swell condition when v_{sab} swells from nominal voltage to 270 V. The series active filter injects appropriate voltage to regulate voltage at load side at its nominal value of 220 V. There is a reduction in grid current during voltage swell condition and rise in grid current during voltage sag condition in order to maintain active power balance.

Fig. 14 shows the performance of the system under load unbalancing condition. The signals captured are DC-bus voltage (V_{dc}), grid current of phase 'b' (i_{sb}), shunt active filter current of phase 'b' (i_{SHb}) and load current of phase 'b'. Fig. 14(a) shows the performance when phase 'b' load is completely removed and Fig. 14(b) shows the performance when phase 'b' load is included. It can be observed under both these conditions, the phase 'b' grid current is maintained sinusoidal and DC-bus voltage is regulated during this disturbance. There is an increase in injected current when the load is removed.

This article has been accepted for publication in a future issue of this journal, but has not been fully edited. Content may change prior to final publication. Citation information: DOI 10.1109/TII.2017.2778346, IEEE Transactions on Industrial Informatics

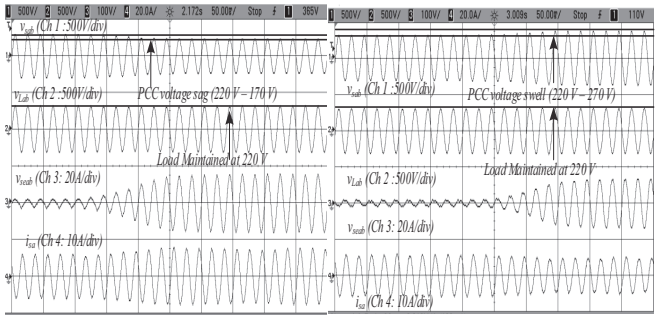

(a) PV-UAPF Operation during Voltage Sag at PCC

(b) PV-UAPF Operation During Voltage Swell at PCC

Fig. 13. PV-UAPF Response under Voltage Sag/Swell Condition at PCC

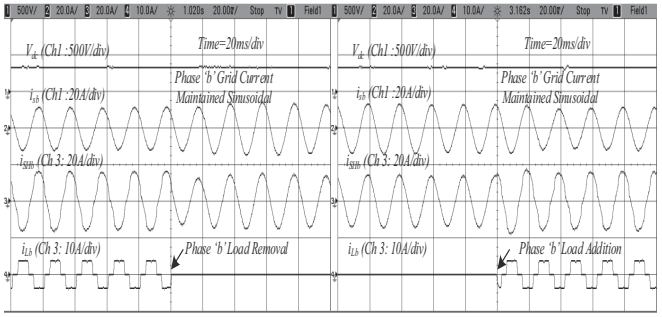

(a) Performance of PV-UAPF under Load Removal in a Phase of the System

(b) Performance of PV-UAPF under Load Addition in a Phase of the System

Fig. 14. PV-UAPF Response under Load Unbalancing Condition

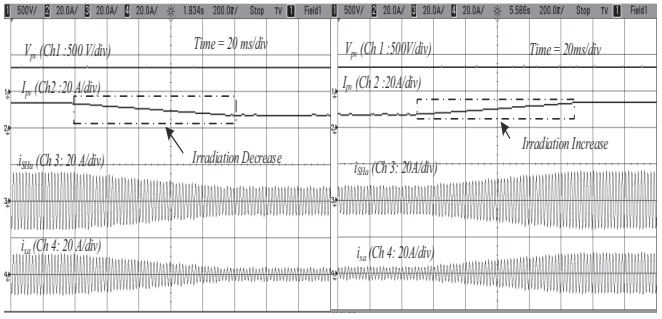

(a) PV-UAPF Response under Reducing Solar Irradiation Condition

(b) PV-UAPF Response under Increasing Solar Irradiation Condition

Fig. 15. PV-UAPF Operation During Change in Solar Irradiation

This is due to the decrease in the load, the extra PV array power is injected into the grid.

The PV-UAPF system behavior during conditions of varying solar irradiation, is presented in Fig. 15. The performance of the system is captured under two conditions i.e. performance under irradiation decrease from 1000 W/m^2 to 500 W/m^2 as shown in Fig. 15(a) and performance under irradiation increase from 500 W/m^2 to 1000 W/m^2 as shown in Fig. 15(b). It can be observed that DC-bus voltage is stable under both these conditions. The MPPT performance under irradiation conditions of 500 W/m^2 and 1000 W/m^2, is given in Fig. 16. It can be observed that the MPPT efficiency is above 99% under both these conditions.

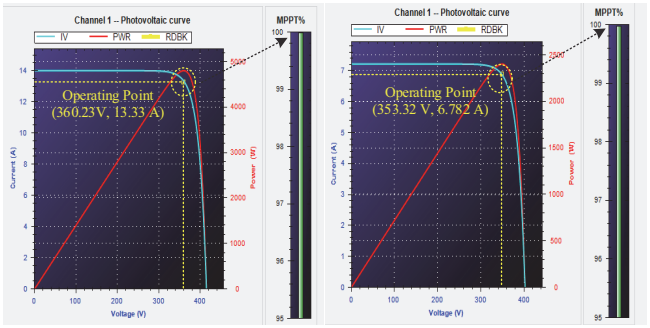

(a) PV-UAPF Maximum Power Point Tracking Performance at 500W/m^2

(b) PV-UAPF Maximum Power Point Tracking Performance at 1000W/m^2

Fig. 16. PV-UAPF Maximum Power Point Tracking Efficiency under Different Irradiation Conditions

D. Performance under Fault Conditions

The operation of the system under three phase short circuit is presented in Fig. 17. Simulated performance is presented due to limitation of hardware experimentation of fault condition in laboratory environment. The system control is implemented such that, the gating to the system automatically shuts down in the event of fault. It can be seen from Fig.17 that a fault occurs at PCC from t=0.3s to t=0.36s The PCC voltage is limited to drop across the short circuit impedance. It can be observed that during this instant though PCC current $i_s(A)$ rises to large value, the load current is nearly zero. The PV array power (P_{pv}) also reduces to zero as the PV-UAPF gating is shunt down. Once the fault is cleared, the PV array power delivered, rises to the nominal conditions and the DC-link voltage is regulated to its desired value of 360 V.

Under conditions of DC-bus faults, the miniature circuit breaker (MCB) in PV array as well as the short circuit protection available in the gate drive circuitry, operate to protect the system. Moreover, the gate driver circuitry provides deadband between switches of the same of the active power filter to prevent shoot through fault. The deadband can be further modified using the dSPACE-Matlab Blocksets to obtain desired deadband duration.

V. Conclusion

The performance of adaptive filter based PV-UAPF system under both steady state and dynamic conditions, have been analyzed in detail. The method of sampling the fundamental component of load current obtained through adaptive filter enables fast extraction of fundamental active component of nonlinear load currents for all phases in one sampling. Only two adaptive filters are required to extract magnitude of active component of three phase load currents. This technique requires reduced computational resources while achieving good dynamic and steady state performance in extraction of fundamental active component of nonlinear load current. The system performance has been found to be satisfactory under various disturbances in load current, PCC voltage and solar irradiation. The series active filter is able to regulate load voltage at 220 V under variations of PCC voltage from 170 V to 270 V. The grid

This article has been accepted for publication in a future issue of this journal, but has not been fully edited. Content may change prior to final publication. Citation information: DOI 10.1109/TII.2017.2778346, IEEE Transactions on Industrial Informatics

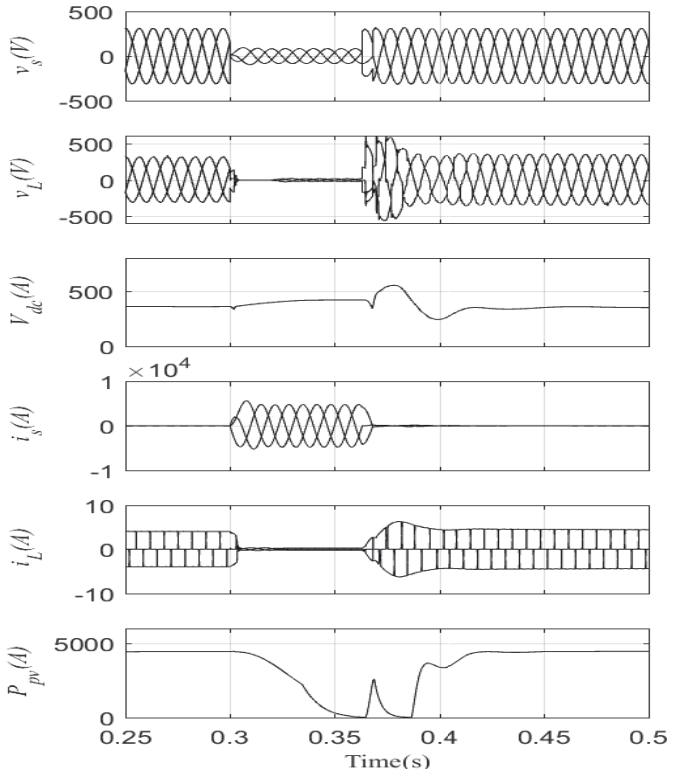

Fig. 17. Performance of PV-UAPF Under Three Phase Short Circuit Fault

current THD is maintained at approximately 3% even though the THD of load current is 28% thus meeting requirement of IEEE-519 standard. The PV-UAPF system has been able to maintain the grid currents balanced under unbalanced loading condition.

The proposed topology and algorithm are suited for employing in conditions where PCC voltage sags/swells and load current harmonics are major power quality issues. Certain power quality issues not addressed include voltage distortions, flicker, neutral current compensation etc. This power quality issues can be addressed by modification of topology and control algorithm according to the requirements in the distribution system.

The PV-UAPF system provides dual benefit of distributed generation as well as improving power quality of the distribution system.

ACKNOWLEDGMENT

This work was sponsored by DST, Govt. of India under Grant Number: RP02979. The authors also thank CSIR-CEERI, Pilani for support during this research work.

REFERENCES

[1] N. R. Tummuru, M. K. Mishra, and S. Srinivas, "Dynamic energy management of hybrid energy storage system with high-gain pv converter," *IEEE Transactions on Energy Conversion*, vol. 30, no. 1, pp. 150–160, March 2015.

[2] B. Singh, A. Chandra, K. A. Haddad, *Power Quality: Problems and Mitigation Techniques*. London: Wiley, 2015.

[3] S. Devassy and B. Singh, "Control of solar photovoltaic integrated upqc operating in polluted utility conditions," *IET Power Electronics*, vol. 10, no. 12, pp. 1413–1421, Oct 2017.

[4] S. Devassy and B. Singh, "Performance analysis of proportional resonant and adaline-based solar photovoltaic-integrated unified active power filter," *IET Renewable Power Generation*, vol. 11, no. 11, pp. 1382–1391, 2017.

[5] L. Ramya and J. Pratheebha, "A novel control technique of solar farm inverter as pv-upfc for the enhancement of transient stability in power grid," in *2016 International Conference on Emerging Trends in Engineering, Technology and Science (ICETETS)*, Feb 2016, pp. 1–7.

[6] R. Stalin, S. S. Kumar, and K. A. R. Fathima, "Coordinated control of upfc with smes and sfcl for improvement of power system transient stability," in *2016 Second International Conference on Science Technology Engineering and Management (ICONSTEM)*, March 2016, pp. 276–280.

[7] R. I. Bojoi, L. R. Limongi, D. Roiu, and A. Tenconi, "Enhanced power quality control strategy for single-phase inverters in distributed generation systems," *IEEE Trans. Power Electron.*, vol. 26, no. 3, pp. 798–806, March 2011.

[8] B. Singh, P. Jayaprakash, D. P. Kothari, A. Chandra, and K. A. Haddad, "Comprehensive study of dstatcom configurations," *IEEE Transactions on Industrial Informatics*, vol. 10, no. 2, pp. 854–870, May 2014.

[9] S. Devassy and B. Singh, "Design and performance analysis of three phase solar PV integrated UPQC," *IEEE Trans. Ind. Appl.*, vol. PP, no. 99, pp. 1–1, 2017.

[10] S. Devassy and B. Singh, "Modified pq-theory-based control of Solar-PV-Integrated UPQC-S," *IEEE Trans. Ind. Appl.*, vol. 53, no. 5, pp. 5031–5040, Sept 2017.

[11] V. Khadkikar, "Enhancing electric power quality using UPQC: A comprehensive overview," *IEEE Trans. Power Electron.*, vol. 27, no. 5, pp. 2284–2297, May 2012.

[12] R. S. Herrera and P. Salmeron, "Instantaneous reactive power theory: A reference in the nonlinear loads compensation," *IEEE Trans. Ind. Electron.*, vol. 56, no. 6, pp. 2015–2022, June 2009.

[13] R. Adda, O. Ray, S. K. Mishra, and A. Joshi, "Synchronous-reference-frame-based control of switched boost inverter for standalone dc nanogrid applications," *IEEE Trans. Power Electron.*, vol. 28, no. 3, pp. 1219–1233, March 2013.

[14] S. Deo, C. Jain, and B. Singh, "A PLL-Less scheme for single-phase grid interfaced load compensating solar PV generation system," *IEEE Transactions on Industrial Informatics*, vol. 11, no. 3, pp. 692–699, June 2015.

[15] B. Singh, K. Kant, and S. R. Arya, "Notch filter-based fundamental frequency component extraction to control distribution static compensator for mitigating current-related power quality problems," *IET Power Electronics*, vol. 8, no. 9, pp. 1758–1766, 2015.

[16] P. Rodriguez, A. V. Timbus, R. Teodorescu, M. Liserre, and F. Blaabjerg, "Flexible active power control of distributed power generation systems during grid faults," *IEEE Trans. Ind. Electron.*, vol. 54, no. 5, pp. 2583–2592, Oct 2007.

[17] Y. F. Wang and Y. W. Li, "Three-phase cascaded delayed signal cancellation pll for fast selective harmonic detection," *IEEE Trans. Ind. Electron.*, vol. 60, no. 4, pp. 1452–1463, April 2013.

[18] R. Kumar, B. Singh, D. T. Shahani, and C. Jain, "Dual-tree complex wavelet transform-based control algorithm for power quality improvement in a distribution system," *IEEE Trans. Ind. Electron.*, vol. 64, no. 1, pp. 764–772, Jan 2017.

[19] H. Dirik and M. Ozdemir, "New extraction method for active, reactive and individual harmonic components from distorted current signal," *IET Generation, Transmission Distribution*, vol. 8, no. 11, pp. 1767–1777, 2014.

[20] M. Srinivas, I. Hussain, and B. Singh, "Combined lms-lmf based control algorithm of dstatcom for power quality enhancement in distribution system," *IEEE Trans. Ind. Electron.*, vol. 63, no. 7, pp. 4160–4168, July 2016.

[21] G. Pathak, B. Singh, and B. K. Panigrahi, "Control of wind-diesel microgrid using affine projection-like algorithm," *IEEE Transactions on Industrial Informatics*, vol. 12, no. 2, pp. 524–531, April 2016.

[22] F. Tedesco, A. Casavola, and G. Fedele, "Unbiased estimation of sinusoidal signal parameters via discrete-time frequency-locked-loop filters," *IEEE Transactions on Automatic Control*, vol. 62, no. 3, pp. 1484–1490, March 2017.

[23] N. Femia, G. Petrone, G. Spagnuolo, and M. Vitelli, "Optimization of perturb and observe maximum power point tracking method," *IEEE Transactions on Power Electronics*, vol. 20, no. 4, pp. 963–973, July 2005.

This article has been accepted for publication in a future issue of this journal, but has not been fully edited. Content may change prior to final publication. Citation information: DOI 10.1109/TII.2017.2778346, IEEE Transactions on Industrial Informatics

REFERENCES

[1] N. R. Tummuru, M. K. Mishra, and S. Srinivas, "Dynamic energy management of hybrid energy storage system with high-gain pv converter," *IEEE Transactions on Energy Conversion*, vol. 30, no. 1, pp. 150–160, March 2015.

[2] B. Singh, A. Chandra, K. A. Haddad, *Power Quality: Problems and Mitigation Techniques*. London: Wiley, 2015.

[3] S. Devassy and B. Singh, "Control of solar photovoltaic integrated upqc operating in polluted utility conditions," *IET Power Electronics*, vol. 10, no. 12, pp. 1413–1421, Oct 2017.

[4] S. Devassy and B. Singh, "Performance analysis of proportional resonant and adaline-based solar photovoltaic-integrated unified active power filter," *IET Renewable Power Generation*, vol. 11, no. 11, pp. 1382–1391, 2017.

[5] L. Ramya and J. Pratheebha, "A novel control technique of solar farm inverter as pv-upfc for the enhancement of transient stability in power grid," in *2016 International Conference on Emerging Trends in Engineering, Technology and Science (ICETETS)*, Feb 2016, pp. 1–7.

[6] R. Stalin, S. S. Kumar, and K. A. R. Fathima, "Coordinated control of upfc with smes and sfcl for improvement of power system transient stability," in *2016 Second International Conference on Science Technology Engineering and Management (ICONSTEM)*, March 2016, pp. 276–280.

[7] R. I. Bojoi, L. R. Limongi, D. Roiu, and A. Tenconi, "Enhanced power quality control strategy for single-phase inverters in distributed generation systems," *IEEE Trans. Power Electron.*, vol. 26, no. 3, pp. 798–806, March 2011.

[8] B. Singh, P. Jayaprakash, D. P. Kothari, A. Chandra, and K. A. Haddad, "Comprehensive study of dstatcom configurations," *IEEE Transactions on Industrial Informatics*, vol. 10, no. 2, pp. 854–870, May 2014.

[9] S. Devassy and B. Singh, "Design and performance analysis of three phase solar PV integrated UPQC," *IEEE Trans. Ind. Appl.*, vol. PP, no. 99, pp. 1–1, 2017.

[10] S. Devassy and B. Singh, "Modified pq-theory-based control of Solar-PV-Integrated UPQC-S," *IEEE Trans. Ind. Appl.*, vol. 53, no. 5, pp. 5031–5040, Sept 2017.

[11] V. Khadkikar, "Enhancing electric power quality using UPQC: A comprehensive overview," *IEEE Trans. Power Electron.*, vol. 27, no. 5, pp. 2284–2297, May 2012.

[12] R. S. Herrera and P. Salmeron, "Instantaneous reactive power theory: A reference in the nonlinear loads compensation," *IEEE Trans. Ind. Electron.*, vol. 56, no. 6, pp. 2015–2022, June 2009.

[13] R. Adda, O. Ray, S. K. Mishra, and A. Joshi, "Synchronous-reference-frame-based control of switched boost inverter for standalone dc nanogrid applications," *IEEE Trans. Power Electron.*, vol. 28, no. 3, pp. 1219–1233, March 2013.

[14] S. Deo, C. Jain, and B. Singh, "A PLL-Less scheme for single-phase grid interfaced load compensating solar PV generation system," *IEEE Transactions on Industrial Informatics*, vol. 11, no. 3, pp. 692–699, June 2015.

[15] B. Singh, K. Kant, and S. R. Arya, "Notch filter-based fundamental frequency component extraction to control distribution static compensator for mitigating current-related power quality problems," *IET Power Electronics*, vol. 8, no. 9, pp. 1758–1766, 2015.

[16] P. Rodriguez, A. V. Timbus, R. Teodorescu, M. Liserre, and F. Blaabjerg, "Flexible active power control of distributed power generation systems during grid faults," *IEEE Trans. Ind. Electron.*, vol. 54, no. 5, pp. 2583–2592, Oct 2007.

[17] Y. F. Wang and Y. W. Li, "Three-phase cascaded delayed signal cancellation pll for fast selective harmonic detection," *IEEE Trans. Ind. Electron.*, vol. 60, no. 4, pp. 1452–1463, April 2013.

[18] R. Kumar, B. Singh, D. T. Shahani, and C. Jain, "Dual-tree complex wavelet transform-based control algorithm for power quality improvement in a distribution system," *IEEE Trans. Ind. Electron.*, vol. 64, no. 1, pp. 764–772, Jan 2017.

[19] H. Dirik and M. Ozdemir, "New extraction method for active, reactive and individual harmonic components from distorted current signal," *IET Generation, Transmission Distribution*, vol. 8, no. 11, pp. 1767–1777, 2014.

[20] M. Srinivas, I. Hussain, and B. Singh, "Combined lms-lmf based control algorithm of dstatcom for power quality enhancement in distribution system," *IEEE Trans. Ind. Electron.*, vol. 63, no. 7, pp. 4160–4168, July 2016.

[21] G. Pathak, B. Singh, and B. K. Panigrahi, "Control of wind-diesel microgrid using affine projection-like algorithm," *IEEE Transactions on Industrial Informatics*, vol. 12, no. 2, pp. 524–531, April 2016.

[22] F. Tedesco, A. Casavola, and G. Fedele, "Unbiased estimation of sinusoidal signal parameters via discrete-time frequency-locked-loop filters," *IEEE Transactions on Automatic Control*, vol. 62, no. 3, pp. 1484–1490, March 2017.

[23] N. Femia, G. Petrone, G. Spagnuolo, and M. Vitelli, "Optimization of perturb and observe maximum power point tracking method," *IEEE Transactions on Power Electronics*, vol. 20, no. 4, pp. 963–973, July 2005.

Sachin Devassy (S'15, M'17) received B. Tech in Electrical and Electronics Engineering in 2007 from Govt. Engineering College, Thrissur, Kerala, India. He received M. Tech in Power Electronics, Electrical Machines and Drives from IIT Delhi in 2010. He is currently working towards his PhD degree in the Department of Electrical Engineering, IIT Delhi, New Delhi, India. He has been working in Power Electronics Group at CSIR-CEERI since July 2010. His areas of research interest include power electronics, power quality, custom power devices and renewable energy systems.

Bhim Singh (SM'99, F'10) was born in Rahamapur, Bijnor, UP, India, in 1956. He received the B.E. degree in electrical from the University of Roorkee, Roorkee, India, in 1977, and the M.Tech. degree in power apparatus and systems and the Ph.D. degree in electrical machine from Indian Institute of Technology (IIT) Delhi, New Delhi, India, in 1979 and 1983, respectively. In 1983, he joined the Department of Electrical Engineering, University of Roorkee (now IIT Roorkee), as a Lecturer. He became a Reader there in 1988. In December 1990, he joined the Department of Electrical Engineering, IIT Delhi, as an Assistant Professor, where he has become an Associate Professor in 1994 and a Professor in 1997. He has been the Head in the Department of Electrical Engineering, IIT Delhi, from July 2014 to August 2016. He is currently the Dean, Academics with IIT Delhi. He has guided 70 Ph.D. dissertations, 161 M.E./M.Tech./M.S.(R) thesis. He has executed more than 75 sponsored and consultancy projects. His areas of research interests include PV grid interface systems, microgrid, power quality, PV water pumping systems, power electronics, electrical machines, drives, FACTS, and HVdc systems.